Fiber array-to-photonic-chip fixation and fine tuning using laser support adjustment

Fiber Array-to-Photonic-Chip Fixation and Fine Tuning Using Laser Support Adjustment

Johan H. C. van Zantvoort, Giok-Djan Khoe, *Fellow, IEEE*, and Huig de Waardt

***Abstract*—A concept for coupling lensed fiber arrays to photonic optical chips in the submicrometer range by using metal deformation is presented. Fine-tuning is possible despite already secured positions between the parts due to precisely chosen step-by-step deformations in the constructions. The smallest fine-tuning step of 0.1 μm is measured using laser support adjustment. The system is packaged and can be temperature controlled. At a constant chip temperature of 22 °C, the package is successfully tested at an ambient temperature range of 0 °C to 60 °C.**

***Index Terms*—Laser adjustment, laser welding, lensed fiber array, packaging, photonic chip.**

I. Introduction

FOR third-generation (3G) photonics technology monolithic integrated components, indium phosphide (InP) is the ideal substrate material for photonic integrated circuits (PICs). Due to the high refractive index, more functionalities by unit area can be processed. Both passive and active optical components can be integrated on one single chip and InP is suited for integration of electrical circuits. By integration of high electron mobility transistors (HEMTs) or hetrojunction bipolar transistors (HBTs) in combination with optical components, PICs operating at bit rates up to 100 Gb/s might be feasible. Examples of optical components are arrayed waveguide gratings (AWGs) for (de)multiplexers, modulators, switches, and couplers (passive components) and laser diodes, photodetectors, and semiconductor optical amplifiers (SOAs) (active components). Combining both active and passive components leads to complicated integrated devices such as optical cross connects (OXC), optical add–drop multiplexers (OADMs), multiple-wavelength lasers, multiple-wavelength receivers, and wavelength converters.

The cost of commercial optical devices is 60%–80% determined by the packaging cost of the bare chip. In particular, the expensive fiber pigtailing operation is the bottleneck for reducing the packaging costs. For multichannel InP-based PICs, the fiber-to-waveguide connection is much more complicated compared to single-fiber devices.

Technological challenges to reduce the coupling loss between standard fibers and waveguides, alignment of several fibers in a small package, and reliable fixation of the fibers in the submicrometer range during its lifetime are important issues.

Manuscript received July 22, 2002; revised September 27, 2002. This work was supported by the Netherlands Organization for Scientific Research (NWO) through the "NRC photonics" grant and the IST-1999–10402 METEOR project.

The authors are with the COBRA Research Institute, Eindhoven University of Technology, 5600 MB Eindhoven, The Netherlands.

Digital Object Identifier 10.1109/JSTQE.2002.806688

First, due to the high index contrast between InP-based waveguides and monomode fibers, mode matching is necessary to reduce losses in mode mismatch between single-mode fibers (8-μm core diameter) and waveguides (typical dimensions 2 μm$\times$ 0.6 μm). For simple fiber butt coupling, the losses are about 10 dB; therefore on-chip spot size converters (SSCs) are needed [1], [2]. Reviews of SSCs are given in [3], [4]. Micro lenses can be assembled between cleaved fiber arrays and photodetector arrays [5], [6] or an optical micro-bench can be monolithically integrated to photodetectors [7]. A section of graded index fiber can be spliced to a single-mode fiber, which acts as a lens [8]. Otherwise, the fiber tip can be lensed to couple light in standard waveguides. In [9], a laser diode is reported integrated with a micro lens on its emitting surface.

Second, there is almost no spatial margin to align the fibers individually in front of the waveguides. Therefore, fibers are usually mounted in V-groove chips [10]–[13]. However, companies worldwide cannot guarantee high-precision lensed fiber arrays with focused infrared (IR) spot positions of exactly 250 μm in the lateral direction and without any height difference in transversal direction. The deviation of the IR spot is on the order of 1-3 μm. This is mainly caused by the lens eccentricity of each individual fiber tip (a typical specification is smaller than 0.5–2 μm). The tolerances on the spacing in the V-grooves (250 ± 0.5 μm) and the assembly method in the V-groove chip, where most frequently adhesives are used that also influence the accuracy of the fiber array.

The third challenge is the fixation of the used components. Laser welding is presently acknowledged as the most stable technology for fixation of fibers and aspherical lenses in fiber optoelectronics [14], [15]. During the welding process, the solidification shrinkage of the welded parts causes misalignment of the components [16]–[18]. Laser beam balance and symmetry are used to minimize these post-weld-shifts (PWSs). The laser hammering (LH) process that compensates for the PWS is proven to be an effective application for single fiber components. For multichannel devices, LH is effective applied in [19].

In the following, a concept is designed with the possibility to realign a fixing plate in front of the chip facet after PWS effects. The procedure is a safe controlled step-by-step operation, so the possibility of PIC and fiber array damage is reduced to a minimum. To test the concept, a commercially purchased lensed four-fiber array is mounted on the fixing plate to reduce the coupling losses. An InP-based PIC with waveguide loops is used as a test chip. For this purpose the position of the IR spot distribution of the four-fiber array is determined. The optimum coupling efficiency as a function of lateral, transversal, and axial alignment is measured and this optimum position is achieved with

the laser adjusting process. Finally, the mechanical stability of the device is tested.

The paper is organized as follows. In Section II, the design of the fiber-chip coupling is explained. The characterization of the fiber array is given in Secion-III A. In Section III-B, experimental results of the couple efficiency between the characterized fiber array and PIC with waveguide loops are given. Section IV describes the assemble method of the fiber array and PIC, the fixation and laser adjust process and finally the packaging method of the device. The thermal stability of the coupling concept is very important. For example, if an AWG is integrated on the PIC, the chip must be tuned by controlling the temperature to provide wavelength stability with respect to the ITU specifications. Active integrated components produce heat and this must also be transferred from the chip. In all cases the pigtail connection must be stable in the submicrometer range. Two thermal stability experiments are described in Section V: first the temperature of the couple construction inside the package is varied, and second the couple construction inside the package is set at a fixed temperature and the ambient temperature outside the package is varied. Conclusions and recommendations are given in Section VI.

II. Design

Pigtailing encompasses the alignment, optimization, and attachment of an optical fiber to a planar optical chip. If the chip requires multiple fiber connections, usually fibers are mounted in a V-groove substrate. This subassembly must be connected to the input and output waveguides of a planar device. In our design a commercially purchased fiber array is used and laser welding is applied for attachment technology. In this section, we explain the basic principle of the coupling and fixation concept.

The PIC is mounted parallel to the fiber tips of the array, thus three degrees of freedom must be controlled: two in the linear lateral x and transversal y directions and one roll position θ_z of the fiber array in combination of the chip facet. The fiber array and PIC are mounted manually, so it is advisable to control the distance between the fiber array and chip facet also (third linear z direction).

The basic alignment principle in given in Fig. 1(a). The fixation and fine tuning method is illustrated in Fig. 1(b). A number of elementary parts can be discerned: the fiber array alignment submount (FAS,1), three elastic pins (2), the solid world (3, a U-shaped body, not shown), the fiber array (4), the fiber array mounting platform (5), the PIC (6), and the removable auxiliary alignment pins (7a,b,and c).

The alignment procedure will now be described as follows. The lateral x, transversal y, and roll position θ_z of the FAS (1) are defined by three elastic pins (2) with respect to the solid world (3). The fiber array is mounted on a stacked, linear adjustable fiber-array mounting platform (5) located on top of the movable FAS (1). The fiber array can now be aligned on the z axis to the input and output waveguides of the PIC (6), which is already mounted on the solid world (3). After optimization of the distance between the fiber tips (4) and the chip facet (6), part (5) is fixed on part (1).

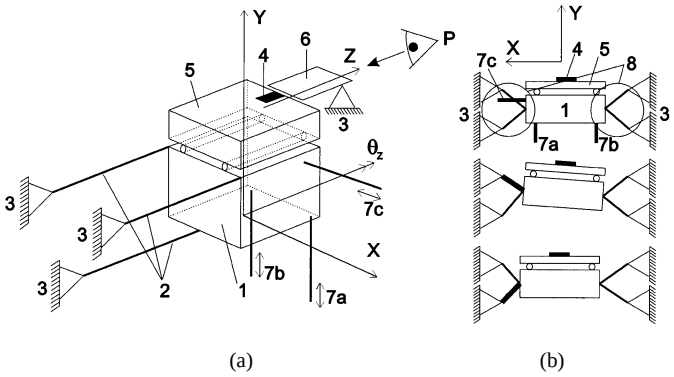

(a) (b)

Fig. 1. (a) Basic alignment principle to control two linear x, y coordinates and one axial θ_z coordinates of the fiber array (4) by using three pins (2), which are connected to the solid world of the device represented by the marks nr. 3. The third linear z direction of the fiber array (4) to the PIC facet (6) can be controlled by a stacked platform (5) on top of the fiber array alignment submount FAS part (1). The position of the fiber array can be controlled by means of three removable pins (7), which are connected to three external piezoelectric actuators. (b) The fine-tuning principle of the fiber array (4) after removal of the displacement pins (7) to the desired position by shrinkage of material in the tuning frames (8).

As mentioned before, the FAS (1) is connected to the solid world by three elastic pins (2). The position of the FAS (1) can be controlled by three removable alignment pins (7a, 7b, and 7c), which are connected to three external piezoelectric actuators. Pin 7a and 7b tilt and roll the array in the vertical y direction, and pin 7c moves it in the horizontal x direction. When the fiber array is aligned in the optimal position with respect to the chip facet, the FAS (1) is welded to the solid world. This procedure is sketched out in Fig. 1(b). The viewpoint is indicated in Fig. 1(a) by point P. Fixation of the x, y, and θ_z position of the FAS (1) is achieved by using two triangular-shaped frames (8), prewelded to the solid world (3). After welding the frames (8) to the FAS (1), the displacement pins 7a, 7b, and 7c are removed.

After the initial welding process, the optimal alignment can get lost due to post welding shift. We can readjust the optimal alignment by using laser trimming of the fixation frames (8). By applying laser welding-induced local heat, the arms of the frames will shrink, which can be utilized for the fine alignment of the fiber array. In Fig. 1(b), this procedure is visualized in the middle and the lower figure. If the left upper arm is welded, the align part is moved to the positive x direction and rotated clockwise. If the left lower arm is welded, the align part is moved in the positive x direction and rotated counterclockwise. Experiments verify that movements in an area of at least 4 μm$\times$ 4 μm lateral and transversal fine-tuning are possible. The amount of laser weld energy is a measure for the displacement.

In Fig. 2, the previously described concept is given in a realized design. The solid platform consists of a U-shaped framed (3) and PIC mounting platform (6). The selected material is invar because of the low linear coefficient of expansion. The fiber-array alignment submount (FAS) (1) is located inside the U-shaped frame and connected with 3 tampon elastic steel pins (2) to the solid platform (only two pins are visible). The fiber array mounting plate (5) is located on top of the FAS (1). This plate can be shifted linearly to the PIC input and output couple facet on two sliding bars at the FAS and is held temporarily in position by a spring. The whole assembly is mounted unambiguously in a fixed position in a piezoelectric aligning operating

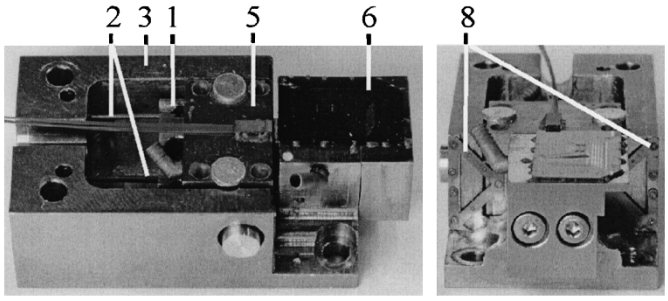

(a) (b)

Fig. 2. (a) Side view and (b) front view of the realized design for fiber-array pigtailing. The design consists of a solid U-shapes frame (3) and PIC mounting platform (6). The fiber array is mounted on the fiber array mounting platform (5), which is stacked on the fiber-array alignment submount (FAS) (1). This is connected to the solid U-shaped frame by three pins (2) (only two pins are visible). Alignment is possible by welding precisely chosen positions on the tuning frames (8).

tool. This tool connects the FAS with three external piezoelectric actuators by three removable displacement pins. Two pins tilt and roll the FAS in transversal and axial directions, respectively, and one pin moves it in a lateral direction. On the operating tool, the fiber-array mounting plate can be connected temporarily with a differential micrometer to control the fiber-array mounting plate on the FAS in the z direction. This connection will be removed after fixation of the fiber-array mounting plate to the FAS. After alignment of the fiber array to the chip facet, the FAS is secured to the solid platform by two tuning frames (8) simultaneously. Those frames are already welded to the solid platform. The material of the tuning frames is steel band because of its resilient property. Fine-tuning is possible by welding the arms of the frames.

In conclusion, the pigtailing concept consists of the following procedure.

- Mounting of PIC and fiber array at a safe distance ($\pm$5 mm) between fiber tips and chip facet.
- Fixation of the optimum distance between used lensed fiber tips and chip facet (20 μm, z direction).
- First alignment of the fiber array in the lateral x direction, transversal y direction, and axial roll θ_z positions using temporary mounted external piezoelectric actuators.
- Securing of the fiber array of the first alignment step, using laser welding by means of two tuning frames.
- Removing piezoelectric actuators.
- Fine-tuning of the fiber array using a step-by-step deformation of the tuning frames with a laser beam.

The previous design is tested with a fiber array of four lensed fibers, the PIC is actually an optical cross-connect chip but there are also waveguide loops integrated. Because the alignment is an active alignment process, both components are characterized before pigtailing.

III. Preliminarily Characterization

As mentioned in the introduction, the IR spot deviation from a standard pitch of 250 μm is on the order of 1-3 μm. Active fine-tuning by monitoring the optimum transmission is necessary for the alignment of the fiber array to the chip facet. For determining in which direction the fiber array has to be aligned, the transmission characteristics of the used components must exactly be known. Therefore, two characterization measurements are carried out. The IR spot positions of the fiber array is determined and the transmission curves in lateral x translation and transversal y translation as a function of the fiber array roll θ_z position is measured. Also, the influence of the other two axial translations pitch θ_x and yaw θ_y positions of the fiber array compared to the PIC is investigated.

A. IR Spot Distribution Measurement of the Fiber Array

The IR spot positions focused by the fiber tips of the fiber array are measured with a movable reference fiber, which is connected to a power meter. When the fiber array is launched with laser light, the maximum measured power corresponds with the IR spot position. The condition is that the reference measure fiber must be controlled with a high resolution in the submicrometer range and it must be translated over a relatively wide range of 750 μm.

In the setup, the fiber array is mounted on a six-axis flexure stage (the linear axis is piezoelectric controlled with active feedback, and the axial axis is controlled manually by differential micrometers). The lensed reference fiber with a lens eccentricity of 0.18 ± 0.08 μm [20] is mounted on a three-axis piezo-controlled stage also with active feedback. This three-axis stage is mounted on a translation stage with a linear encoder. The linear translation stage is automatically controlled by a personal computer for the translation of exactly 250.0 μm. In every motion loop of 50 nm, the absolute position is measured and checked with the desired position. However, due to flatness, straightness, and tilt, systematical errors will be generated. By using an interference measurement rapport of the translation stage, the best position regarding flatness, straightness, and tilt (roll, pitch, and yaw) errors is selected. At this position, the maximum transmitted IR light from the first fiber of the fiber array to the reference fiber is observed and the x and y coordinates of the piezoelectric actuators are noted. The reference fiber is translated over a range of 250 μm to the second fiber of the fiber array and the x and y coordinates are noted again when the maximum transmission occurs. This is repeated for the third and fourth fiber. This procedure was performed at 29 different positions side by side of the stage. Each position has an offset of 250.0 compared to the previous position.

All of the x and y positions of the four fibers of these 29 measurements are compared with each other and the absolute IR spot positions and the population standard deviation of all observations in lateral x and transversal y direction are given in Figs. 3 and 4, respectively. In Fig. 5, the fiber array with the used fiber numbering is given. From Fig. 3, it can be concluded that the IR spot pitch between fibers 1 and 2 is 248.9 ± 0.6 μm (if the line was horizontal, the pitch was 250 μm). The maximum measured transmitted light in the x position is 1.1 μm in the direction of fiber 1. The pitch between fibers 2 and 3 is also 248.9 ± 0.4 μm and between fibers 3 and 4 the spot pitch is 250.6 ± 0.5 μm. Fibers 1 and 4 will be connected to a waveguide loop and fibers 2 and 3 will be connected. The pitch between fiber pair 1-4 is 750 μm minus the difference between fibers 1 and 4 in the lateral x direction. This is equal to 748.4 ± 0.7 μm. The pitch between fibers 2 and 3 is 248.9 ± 0.4 μm. In Fig. 4,

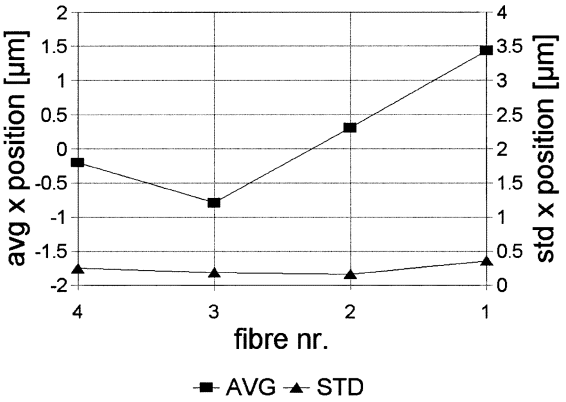

Fig. 3. Measured average IR spot positions and population standard deviation of 29 observations in lateral x direction.

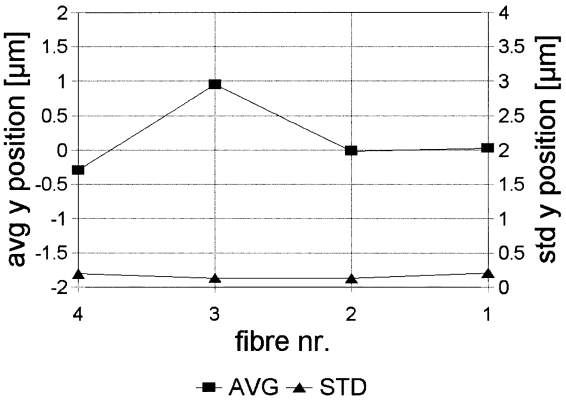

Fig. 4. Measured average IR spot position and standard population deviation of 29 observations in the transversal y direction.

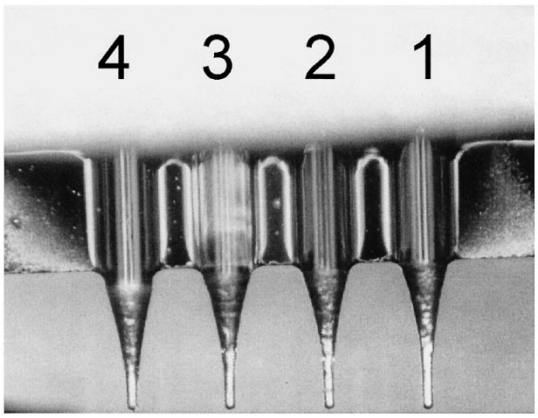

Fig. 5. Photograph and fiber numbering of the fiber array used in this paper.

it can be seen that the IR spot of fiber 3 has a deviation of 1 μm in the transversal y direction. The positions of the measured IR spots and the probability intervals are shown schematically in Fig. 6. The four crosses indicate the desired IR spot positions at pitches of 250 μm. The four rectangles are the probability areas where the actual IR spot positions are located taking fiber nr. 1. as reference. In the figure, the deviation of the desired position and actual measured position compared with fiber 1 are given in micrometers. From this view, it is obvious that there must be three optimum positions of the fiber array compared to the waveguide loops of the PIC (dotted lines in Fig. 6). After all,

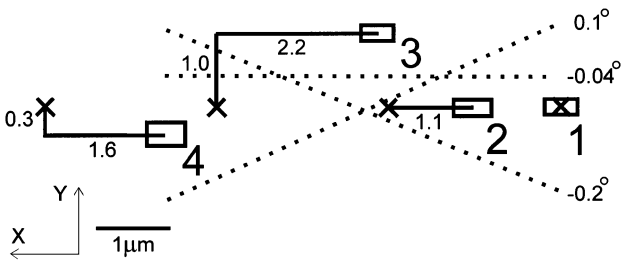

Fig. 6. Presentation of the optimal IR spot positions at pitches of 250 μm (crosses) and the measured IR spot positions with their probability intervals in x-y plane (rectangles). Due to fiber 3, there are three possible optimal position of the fiber array in front of the chip facet (dotted lines).

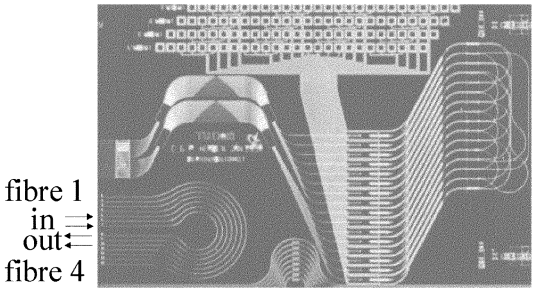

Fig. 7. Optical cross-connect chip including waveguide loops for packaging experiments [21] fibers 1 and 2 are connected to the IN ports, and fibers 3 and 4 are connected to the OUT ports.

fibers 1 and 4 are connected together by a waveguide loop and fibers 2 and 3 are connected with a waveguide loop.

B. Fiber-Array Waveguide Loop Experiments

With the fiber array characterized in the previous section, a number of waveguide loop experiments were carried out. The chip layout is given in Fig. 7 [21]. Fibers 1 and 2 of the array are connected to a laser source and IR light is transmitted in the two IN ports of the chip (see Fig. 7). Fibers 3 and 4 are connected to power meters and measure the power of transmitted light trough the waveguide loops at the OUT ports (Fig. 7). First the optimization in lateral x, transversal y, and roll position θ_z is determined. After this, angular dependence in the coupling efficiency in the pitch θ_x and yaw θ_y of the fiber array in relation to the chip facet is investigated. To find the optimum position of the fiber array, fiber pair 1-4 is optimally aligned. The transmission curve is measured when the PIC is translated over a range of 4 μm in both the lateral and transversal directions. The measured data is stored in a database. The same procedure is repeated for fiber pair 2-3, when the optimum position is set for this combination. This measurement is performed for different θ_z roll positions of the fiber array.

In Fig. 8, the maximum transmission loss of both fiber-pair combinations as a function of the roll position is given when fiber pair 1-4 is optimally aligned. In Fig. 9 the same plot is given, but now fiber pair 2-3 is optimaly aligned. There are indeed three optimum positions measured for both fiber pairs. The optimum position of the fiber array at roll position -0.04° if fiber pair 2-3 is aligned optimally is preferred (see Figs. 6 and 9).

The total excess loss for both fiber pairs is 13.5 dB. This is composed of twice the coupling loss as a result of mode mismatch between waveguide dimensions and fiber tip with a ra-

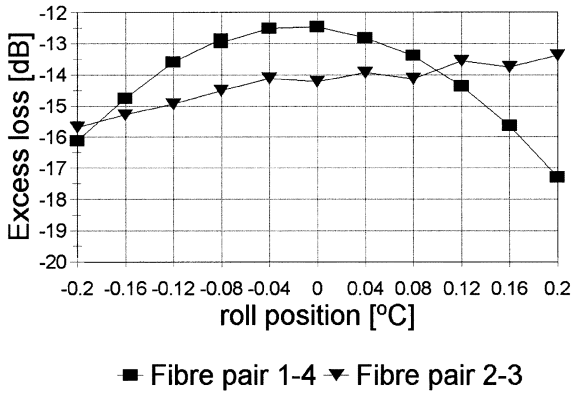

Fig. 8. Transmission characteristics as a function of the fiber-array roll position when fiber pair 1-4 is optimized.

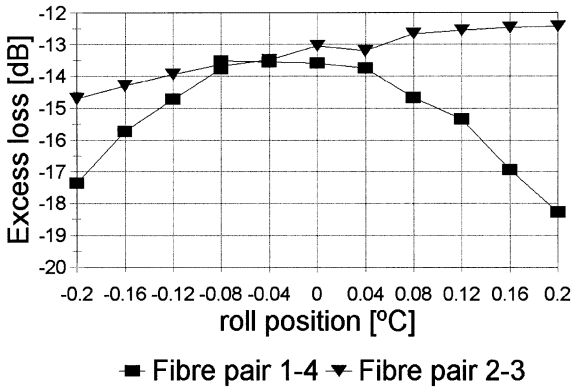

Fig. 9. Transmission characteristics as a function of the fiber-array roll position when fiber pair 2-3 is optimized.

dius of 14 ± 2 μm, which is equal to 8.8 ± 0.8 dB. In [20] this value is determined. The IR spot pitch of both fiber pairs are 748.4 ± 0.7 μm and 248.9 ± 0.4 μm for fiber pairs 1-4 and 2-3, respectively. Both fibers of each pair are located approximately 0.7 μm off axis. In [20], the fiber displacement is measured to be 0.7 μm in lateral direction, and the coupling loss increases with 0.8 dB. The extra coupling losses are 1.6 dB. Moreover, extra coupling losses are contributed due to fiber 3. This fiber has a deviation of 1 μm in the transversal direction. Therefore, the other three fibers must be adjusted, so that the distances of both fiber pairs are the same value of about 0.5 μm. The extra loss increase of 0.5 μm fiber displacement is 0.5 dB, measured in [20]. Total loss increase by compensating the fiber array for fiber 3 is 1 dB. Additionally, another 2 dB is due to waveguide losses of 14-mm waveguide length. In Table I, the reduction contribution to the total loss is given. The most significant contribution of the total loss is the overlap mismatch between the cylindrically focused spot size of the fiber and the elliptical field of the waveguide. This can be reduced by using lensed fibers with a smaller lens radius or by using new types of lensed fibers featuring two different radii of curvature, designed to accommodate elliptical spots. These tapers show a coupling loss of smaller then 1 dB [22].

From all measurements, it is observed that the optimum transmission of each fiber pair individually occurs with a lateral shift of 0.2 μm and a transversal shift of 0.6 μm. This corresponds with the IR spot position determination.

The array is set at a roll position of -0.04 (Fig. 9), and the θ_x pitch position of the array is varied over a range of 6° (3° up and 3° down) compared to the chip. This has no influence on the coupling efficiency. The θ_y yaw position is translated over a total angle of 1.2°, here again 0.6° left and 0.6° right of the parallel position. This is also not crucial for the coupling efficiency. Coupling efficiency as a function of the fiber tips to chip facet distance is investigated. In all observations, there was a difference of about 5 μm in maximum coupling efficiency for both fiber pairs in the z direction, which results in an extra loss of 0.25 dB.

We can conclude from the above that the IR fiber-pair spot pitches of 248.9 ± 0.4 μm and 748 ± 0.7 μm are measured instead of 250.0 μm and 750.0 μm. In the transversal direction, one IR spot position is located 1 ± 0.2 μm off axis in comparison with the other three fibers. As a result, three optimum lateral x, transversal y, and θ_z roll positions of the array are measured. Extra excess loss for both fiber-pair combinations of 2.6 dB is introduced as a result of the quality of the fiber array. The other angle-dependence pitch θ_x and yaw θ_y of the used fiber array with a fiber-tip radius of 14 ± 2 μm are in relation to the chip facet, which is not crucial concerning the coupling efficiencies.

IV. Assembly of the Device

For the alignment and attachment of the characterized fiber array, an operating tool is designed with the possibility to adjust the fiber array with temporary connected piezoelectric actuators. After optimum alignment of the fiber array, fixation using standard laser weld equipment is performed. The couple construction is mounted unambiguously in this piezoelectric align operating tool on three ball grooves in combination with three balls of ruby. The FAS is connected temporary with the piezoelectric actuators by displacement pins and the fiber-array mounting plate is connected with the differential micrometer.

The fiber array is placed centrally on the fiber-array mounting plate (see Fig. 2 nr. 5) and held in position using six vacuum holes. The fiber array is visually aligned to be perpendicular to the mounting plate using a microscope. The array is mounted with thixotropic two components epoxy. After curing, the vacuum hose is uncoupled from the mounting plate. The same procedure is repeated for the PIC. The chip is visually aligned adjusting the input and output waveguides to be parallel and opposite to the four fiber tips. The PIC is temporary held in position using vacuum and permanently attached to the PIC platform (Fig. 2 nr. 6) using epoxy. As mentioned in Section II, the fiber-array mounting plate can shift linearly to the chip facet on two sliding bars. The mounting plate is temporarily connected to a differential micrometer, which allows control of the mounting plate on the order of 0.5 μm over a range approximately of 5 mm. The optimum distance between fiber tips and chip facet is 20 μm. The fiber-array mounting plate (Fig. 2 nr. 5) is fixed to the FAS (Fig. 2 nr. 1) by filling the four holes in the border with epoxy (Fig. 2 nr 5). The influence of a possible shrinkage effect in the fiber-chip distance is minimized as the forces in this direction are avoided as a consequence of the perpendicular direction of the holes to the rods. After hardening of the epoxy the differential micrometer is disconnected.

TABLE I
TRANSMISSION LOSS CONTRIBUTION FOR BOTH FIBER-PAIR COMBINATIONS

	Loss [dB]
Mode mismatch between input lensed fibre and wave-guide	4.4
Mode mismatch between wave-guide and output lensed fibre	4.4
Extra losses due to the incorrect I.R. spot pitches of 250 μm	1.6
Extra losses for compensating in transversal direction due to fibre 3	1
Wave-guide losses of 14 mm length average	2
Total loss	13.4

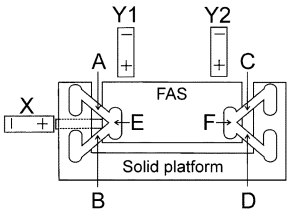

Fig. 10. Laser adjust design. The FAS can align compared to the solid platform by applying laser-welded-induced local heat at positions A, B, C, and D. Y1, Y2, and X are noncontacting displacement transducers.

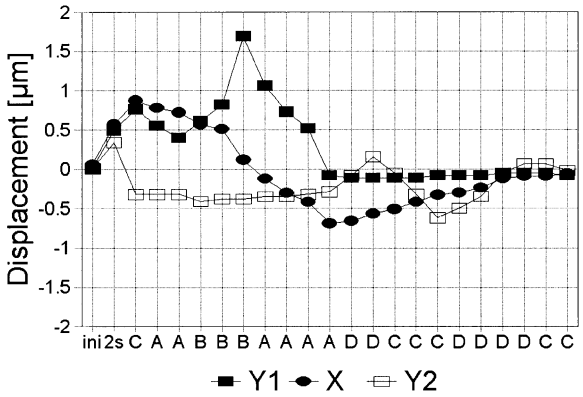

Fig. 11. Laser adjust process. Displacement of the FAS in the Y1, Y2, and X directions (see Fig. 10) as a function of the laser welded part position. Explanation of the x axis: ini is initial position, 2s fixation of the FAS to the solid platform at positions E and F simultaneously and the next positions A, B, C, or D are the welded positions of the tuning plates for the fine-tune alignment to reach the initial state.

The FAS is actively aligned by connecting fibers 1 and 2 to a laser source and reads the measured power of fibers 3 and 4. With the help of a microscope, the FAS is aligned at a roll position parallel to the chip by focusing the FAS ends with the U-shape. The absolute position of the FAS is measured by three noncontacting displacement transducers Y1, Y2, and X (Fig. 10). The relative roll position can be calculated with Y1 and Y2. With the help of Figs. 8 and 9, the preferred position of the fiber array can be set using the external piezoelectric actuators with active feedback. When the optimum position is set, the FAS is laser welded to the chassis at positions E and F simultaneously (Fig. 10).

The laser welder is a 100-W Nd:YAG laser with a pulsewidth of 5 ms. The single laser is provided with an energy share module, which is connected to two 600-μm step-index (SI) optical fibers. These fibers deliver the energy to two focusing heads with a focus length of 100 mm. Both focusing heads are positioned symmetrically and at the same angles compared to the tuning frames. The beam pulse energy for welding at points E and F are 5 J for each welding. After fixation, one focusing head is used for fine tuning the fiber array applying laser adjusting at points A, B, C, and D (see Fig. 10). During this process, the beam pulse energy of the Nd:YAG laser welder is reduced and extra filters are necessary to reduce the beam pulse energy to values in the range 1.1–0.8 J. The dimensions of the cross sections of the arms are 1.2 mm $\times$ 0.2 mm. The welded spot diameter can vary from 1 to 0.5 mm. If the cross section of the arms increase, the align step becomes smaller by the same laser weld energy. The align area is a function of the arm lengths. In Fig. 11, the fixation and fine-tune laser adjust process is shown. Initially the fibers are active aligned to the desired inputs and outputs of the PIC (Fig. 11, x axis ini). The noncontacting displacement transducers are reset and both tuning frames, which are already welded to the chassis, are now welded to the FAS. Due to the PWS, the flexible part is shifted 0.5 μm in the transversal Y and the lateral X directions (Fig. 11, x axis 2s). The external piezoelectric actuators are subsequently disconnected. The FAS is tuned back in the negative Y2 direction by laser trimming the fixation frame at point C (see Figs. 10 and 11). Next the FAS is adjusted in the negative lateral x direction by welding points A, A, B, B, and B (see Figs. 10 and 11). The FAS is now adjusted in the negative Y1 direction by welding 4 $\times$ position A (Figs. 10 and 11). Note that the position at Y2 is constant. Y1 is now in the initial position and the FAS must be adjusted in the positive lateral x direction by laser adjusting 2 $\times$ D, 3 $\times$ C, 4 $\times$ D and finally 2 $\times$ at point C (Figs. 10 and 11). The FAS is laser adjusted within 0.1 μm of the initial position.

The couple construction can now be removed from the piezoelectric align operating tool and mounted in package made of brass (Fig. 12). The couple construction is mounted on a 10.6-W thermo electric cooler (TEC). The temperature is measured by an NTC miniature thermistor for a quick response. Commercially purchased four-pin feed troughs are soldered in the package for electrical interconnection (Fig. 12 nr. 1). The fibers are guided trough a feed-trough aperture. Two conical half-round enclosure caps made of rubber seals the feed-trough aperture by tightening the outer flange (Fig. 12 nr 2). Two gas faucets (3) are made in the package for filling the device with dry nitrogen. A precision O-ring (4) is used to seal the package with a lid. The package is tested with a helium leak tester at a pressure of 10^{-9} Pa. No leak was observed. Finally, the package is filled with dry nitrogen using the gas faucets.

With this proof-of-principle experiment, the basic concept of Section II is demonstrated with the characterized fiber array of Section III and test PIC, and the maximum feasible couple effi-

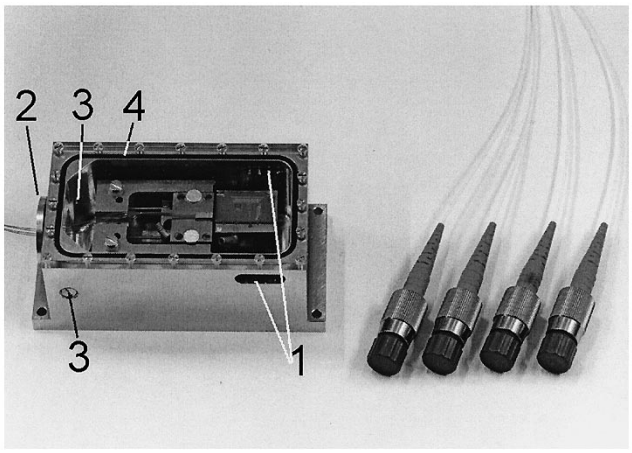

Fig. 12. Couple construction mounted on a TEC in a hermetic closed package and filled with dry nitrogen gas. Dimensions: 7 cm (l) × 4 cm (b) × 3 cm (h).

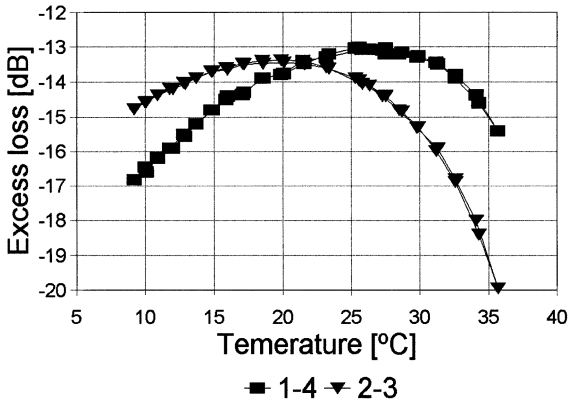

Fig. 13. Transmission characteristics between fiber-pair combinations 1-4 and 2-3 as function of temperature of the couple construction inside the package.

ciency (measured also in Section III) is achieved by laser-supported fine-tune adjustment. The system is hermetically packaged and the package is filled with dry nitrogen gas to avoid water condensation at low temperatures of the construction inside the package.

V. Thermal Stability Experiments

As mentioned in the Introduction, the thermal management of InP-based components is very important. Most optical PICs have to be tuned by setting the chip temperature to an operating value, so it is important that the design is mechanically stable over a certain temperature range. The couple construction is varied over a range of 10 °C to 35 °C. The FAS is laser adjusted at an ambient temperature of 22 °C. At this temperature, both fiber pairs to waveguide loop combinations have a total excess loss of 13.5 dB (Fig. 13), which is the maximum feasible with the used components as measured in Section III. If the temperature is changed, the total excess loss curve has the same tendency if the PIC is moved in the transversal y direction regarding the fiber array. In the preliminarily measurements, the PIC is translated in the positive y direction (for a definition see Fig. 1). In all graphs, the peak transmission of fiber pair 1-4 is

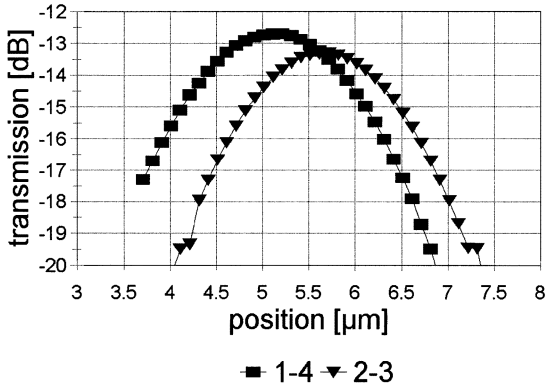

Fig. 14. Transmission characteristics between fibers-pair combinations 1-4 and 2-3 as a function of the transversal y position of the fiber array related to the chip facet.

measured first, followed by fiber pair 2-3 at a distance of 0.6-μm averages. This corresponds with the IR spot position determination of the fiber array (Fig. 6). If the PIC is translated lateral in front of the fiber array, the curves of fiber pairs 1-4 and 2-3 are almost the same but there is a difference in maximal transmission peaks, and those peaks are shifted 0.2 μm. So we can conclude that an offset in the transversal y direction must be introduced if the temperature changes. From all measured curves, the curve given in Fig. 14 is the best fit with the measured curve as a function of ambient temperature (Fig. 13). The curve in Fig. 14 is measured at a fiber-array roll position of -0.04° when fiber pair 2-3 is optimally aligned (Fig. 9) and the chip is moved over a range of 4 μm in the transversal direction. We can conclude that the FAS and fiber-array mounting platform (Fig. 2 nr. 1 and 5) compared to the chip mounting platform (Fig. 2 nr. 6) shifts 0.08 μm/°C. At the position of both peaks, it can be concluded that, if the couple construction is heated up, the FAS and fiber-array mounting platform expands more compared to the PIC mounting platform.

The linear coefficient of expansion of the materials invar, indium phosphide, silicium, and glass are of the same order, namely 10^{-6}. The linear coefficient of expansion of the steel sliding bars between the FAS and fiber-array mounting platform and the tuning frames are on the order of 10^{-5}. The sliding bars have a diameter of 1.5 mm. A 1° temperature increase results in a 0.02-μm expansion. In a redesign, this can easily be avoid. The length of the arms of the tuning plates is 7.5 mm. A 1° temperature increase results in a length increase of 0.08 μm. This will be 0.06 μm in the lateral and transversal directions because the arms of the tuning frames are positioned at an angle of 45° compared to the FAS and PIC mounting platform.

Due to the symmetrical design of the tuning frames, it was expected that the displacement of the FAS compared to the PIC mounting platform as a function of temperature should be zero. Due to the tension between the arms and the solid platform, it is plausible that the arms of the U-shaped frame are bent toward each other. When the temperature increases, the arms of the tuning plates push the U-shaped frame apart. This could explain why the FAS expanded upwards when the temperature increases. In future designs, this can be avoided by proper material choices and redesign of the U-shaped frame.

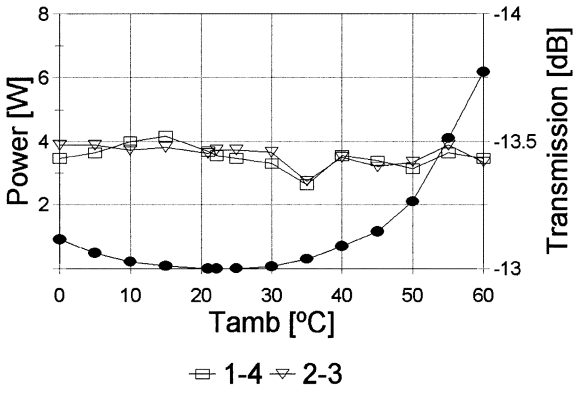

Fig. 15. Transmission characteristics for both fiber pairs 1-4 and 2-3 as a function of ambient temperature outside the package (Y-scale right) and supplied power to the TEC to hold the couple construction at 22 °C inside the package (Y-scale left).

The fiber array and PIC are mounted with corner joints of epoxy. The influence of the epoxy is also an unknown factor.

In a second experiment, the PIC temperature is set at 22 °C. The ambient temperature is varied three times from 0 °C to 60 °C. Fig. 15 gives the measured average excess loss (Y-scale right) and the supplied power to the TEC (Y-scale left). Over the temperature range from 0 °C to 60 °C, the excess loss is 13.4 ± 0.1 dB for both fiber-pairs combinations 1-4 and 2-3. Therefore, the TEC controls the couple construction and chip temperature at a constant temperature of 22 °C at a power of less than 6 W. The measured polarization dependence is about 0.3 dB (propagation loss of 1.2 dB/cm for TE-polarization and 1.5 dB/cm for TM polarization of the on-chip waveguides).

The fiber array is fine-tuned and laser welded to the PIC at an ambient temperature of 22 °C. If the couple construction is tuned to 22 °C the maximum couple efficiency is measured. Heating up or cooling down the couple construction results in a misalignment increase of 0.08 μm/°C. The packaged device can hold the couple construction at a stable temperature of 22 °C by varying the ambient temperature from 0 °C to 60 °C.

VI. Conclusion and Recommendations

For the final proof-of-principle experiment, the IR spot positions of a commercially purchased four-lensed fiber array is measured. IR fiber pair spot pitches of 248.9 ± 0.4 μm and 748 ± 0.7 μm are measured instead of 250.0 μm and 750.0 μm. In the transversal direction, one IR spot position is located 1 ± 0.2 μm off axis by comparison with the other three fibers. As a result, three optimum lateral x, transversal y, and θ_z roll positions of the array are measured. In two situations, excess losses of 13.5 dB are measured. This is the optimum feasible value with the used components. The most significant contribution of the total loss is the overlap mismatch between the cylindrically focused spot size of the fiber and the elliptical field of the waveguide. This can be reduced by using lensed fibers with a smaller lens radius or special fiber tips featuring two different radii of curvature, designed to accommodate elliptical IR spots. Extra excess loss for both fiber-pair combinations of 2.6 dB is introduced as a result of the quality of the fiber array. If the focused IR spot becomes smaller or elliptical, the coupling loss decrease but the axial offset of the fibers individually becomes more critical. The other angle dependences pitch θ_x and yaw θ_y of the used fiber array with a fiber-tip radius of 14 ± 2 μm are in relation to the chip facet and are not crucial with regard to the coupling efficiencies.

The fiber-array coupling design is realized and laser adjusting after permanent fixation is demonstrated. To compensate for PWS, both tuning frames are fixated simultaneously at balanced beam pulse energy of 5 J. PWS on the order of 0.5 μm in both lateral and transversal directions is measured. After the fine-tuning process, the initial position is achieved. The minimum fine-tuning step of the fiber array is 0.1 μm in both the lateral and transversal directions by reducing the laser beam pulse energy to 0.8 J. This fine-tuning step can be smaller by the design of the tuning frames. The dimensions of the cross sections are 1.2×0.2 mm. If the cross section increases, the align step becomes smaller by the same applied laser weld energy. The align area is a function of the arm lengths. In our first prototype, we align the movable part in an area of at least 4 μm$\times$ 4 μm. The arms lengths are about 7.5 mm. This was proven to be effective for our application. Therefore, we did not investigate other dimensions of the tuning frames, but we have identified this topic for further research.

The thermal stability of the couple construction is tested in a range from 10 °C to 35 °C. We measured a misalignment increase of 0.08 μm/°C. This requires active temperature stabilization; however, the PIC needs to be temperature-controlled as well to maintain the specified optical properties.

The couple construction is hermetically packaged and no leak is measured at a vacuum of 10^{-9} Pa. The package is filled with dry nitrogen gas and in this condition the ambient temperature is varied from 0 °C to 60 °C. The couple construction inside the package is held at a constant temperature of 22 °C and the excess loss remains constant.

The design is a good basic principle for manipulation and for fixation of fiber arrays in the submicrometer range. In future devices, we will improve the mechanical stability, so the PICs can be tuned without extra transmission losses and we will optimize the coupling efficiency by applying an aspherical design of lensed fibers. Fiber concentrators will be investigated to reduce waveguide pitches. We will commence fabrication of high-precision fiber arrays. Laser adjusting will also applied for manipulating the fiber array to the PIC facet. Applying pick and place machines for the attachments of fiber arrays and PICs can use this principle as a basic tenet toward more advanced techniques for mass production.

Acknowledgment

The authors would like to thank T. M. Maas and E. C. A. Dekkers for their suggestions and solutions concerning mechanical matters, P. Brinkgreve for the investment in the laser weld equipment. P. W. van den Hoogen for the design and realization of the piezoelectric alignment operating tool, H. J. M. de Laat and J. A. M de Laat for realization of the fiber array PIC couple construction, J. A. Bulsink for making the linear control movement system of the fiber array, R. M. van Teeffelen for the

realization of the package and leak test experiments, and L. C. Cleven for operating the laser weld system.

REFERENCES

[1] G. Wenger, M. Schienle, J. Bellermann, B. Acklin, J. Müller, S. Eichinger, and G. Müller, "Self-aligned package of an 8×8 InGaAsP-InP space switch," *IEEE J. Select. Topics Quantum Electron.*, vol. 3, pp. 1445–1456, Dec. 1997.

[2] J. Stulemeijer, A. F. Bakkker, I. Moerman, F. H. Groen, and M. K. Smit, "InP-based spotsize converter for integration with switching devices," *IEEE Photon. Technol. Lett.*, vol. 11, pp. 81–83, Jan. 1999.

[3] I. Moerman, P. P. van Daele, and P. M. Demeester, "A review on fabrication technologies for monolithic integration of tapers with III-V semiconductor devices," *IEEE J. Select. Topics Quantum Electron*, vol. 3, pp. 1308–1320, Dec. 1997.

[4] B. Mersali, A. Ramdane, and A. Carenco, "Optical-Mode transformer: A III-V circuit integration enabler," *IEEE J. Select. Topics Quantum Electron*, vol. 3, pp. 1321–1331, Dec. 1997.

[5] D. Yap, A. Au, and L. K. Kendall, "Microfixtured assembly for lensed optoelectronics receivers," *IEEE Trans. Adv. Packag.*, vol. 24, pp. 586–589, Nov. 2001.

[6] E. Anderson, D. Tran, R. Strijek, E. Rezek, R. Johnson, J. Klein, D. Boger, G. Uchiyama, and M. Folkman, "Coupling of waveguides to detectors using spherical lenses and lens fibers," in *Proc. LEOS Annual Meeting '98*, vol. 2, 1998, pp. 384–385.

[7] D. Tran, E. Anderson, E. Rezek, R. Strijek, R. Johnson, G. Uchiyama, R. DePacce, L. Rochin, A. Hirschberg, and P. Hurt, "Monolithic integrated optical micro-bench for high density photonics packaging," in *Proc. Electron. Comp. Technol. Conf.*, 1998, pp. 588–589.

[8] P. Chanclou, M. Thual, J. Lostec, P. Auvray, J. Caulet, G. Joulié, A. Poudoulec, and B. Clavel, "Highly efficient collective coupling between laser diode array and lensed fiber ribbon," *Electron. Lett.*, vol. 34, no. 3, pp. 273–274, Feb. 1998.

[9] Y. Fu and N. K. A. Bryan, "A novel one step integration of edge-emitting laser diode with micro-elliptical lens using focused ion beam direct deposition," *IEEE Trans. Semiconduct. Manufact.*, vol. 15, pp. 2–8, Feb. 2002.

[10] T. Kato, F. Yuuki, K. Tanaka, T. Habu, Y. Akiyama, T. Shimura, A. Takai, K. Mizuishi, T. Teraoka, and Y. Motegi, "A new assembly architecture for multichannel single mode-fiber-pigtail LD/PD modules," *IEEE Trans. Comp. Hybrids, Manufact. Technol*, vol. 16, pp. 89–94, Feb 1993.

[11] E. Grard, J. le Bris, M. Di Maggio, F. Dorggeuille, J. Y. Emery, P. Bonno, and M. Renaud, "High performance packaging used for clamped gain semiconductor optical amplifier array modules fabrication," in *Proc. Electr. Components and Tech. Conf.*, 1998, pp. 1270–1273.

[12] J. H. C. van Zantvoort, F. M. Huijskens, C. G. P. Herben, and H. de Waardt, "Fiber array pigtailing and packaging of an InP-based optical cross connect chip," *IEEE J. Select. Topics Quantum Electron*, vol. 5, pp. 1255–1259, Sept./Oct. 1999.

[13] H. Ehlers, M. schlak, and U. H. P. Fischer, "Multi-fiber-coupling modules for monolithically integrated Mach-Zehnder interferometers for TDM/WDM communication systems," in *Proc. Optical Fiber Communication Conf. and Exhibit*, vol. 3, 2001, pp. WDD66-1–WD66-3.

[14] M. K. Song, S. G. Kang, N. Hwang, H. T. Lee, S. S. Park, and K. E. Pyun, "Laser weldability analyzes of high-speed optical transmission device packaging," *IEEE Trans. Comp. Packag., Manufact. Technol. B*, vol. 19, pp. 758–763, Nov 1996.

[15] G. M. Chaoui, J. Lipson, R. S. Moyer, and T. S. Stakelon, "A method of achieving improved radial alignment in an optical package utilizing laser welding techniques," in *Electron. Comp. Conference, 1989. Proceedings.,39th*, 1989, pp. 372–373.

[16] S. C. Wang, H. L. Chang, C. Wang, C. M. Wang, J. W. Liaw, M. T. Sheen, J. H. Kuang, C. P. Chien, G. L. Wang, and W. H. Cheng, "Post-weld-shift in semiconductor laser packaging," in *Proc. 49th Electron. Comp. and Technol. Conf.* , 1999, pp. 1159–1163.

[17] W.-H. Cheng, M.-T. Sheen, C.-P. Chang, and J.-H. Kuang, "Reduction of fiber alignment shifts in semiconductor laser module packaging," *J. Lightwave Technol.*, vol. 18, pp. 842–848, June 2000.

[18] W. H. Cheng, W. H. Wang, Y. M. Huang, H. Y. Chen, and H. H. Lin, "Failure mechanism of hole formation in laser welding technique for optoelectronic packaging," in *Proc. 45th Electron. Comp. and Technol. Conf.*, 1995, pp. 914–916.

[19] S.-G. Kang, M.-K. Song, S.-S. Park, S.-H. Lee, N. Hwang, H.-T. Lee, K.-R. Oh, G.-C. Joo, and D. Lee, "Fabrication of semiconductor optical switch module using laser weling technique," *IEEE Trans. Adv. Packag.*, vol. 23, pp. 672–680, Nov. 2000.

[20] J. H. C. van Zantvoort, C. G. P. Herben, and H. de Waardt, "Multi-fiber to InP-based waveguide coupling efficiency determination," *Proc. 2000 IEEE/LEOS Symp. Benelux Chapter*, pp. 147–150.

[21] C. G. P. Herben, D. H. P. Maat, X. J. M. Leijtens, M. R. Leys, and M. K. Smit, "Polarization independent dilated WDM cross-connect on InP," *IEEE Photon. Technol. Lett.*, vol. 11, pp. 1599–1601, Dec. 1999.

[22] B. Sverdlov, B. Schmidt, S. Pawlik, B. Mayer, and C. Harder, "1 W 980 nm pump modules with very high efficiency," in *Proc. 28th Eur. Conf. on Optical Communication*, 2002, PD3.6, pp. PD3.6–1–PD3.6–3.

Johan H. C. van Zantvoort was born in Riethoven, The Netherlands, on November 21, 1968. He graduated with a degree in applied physics from the Technical College of Eindhoven in 1994.

He was with DAF Trucks Research, Philips Centre for Manufacturing Technology and Philips Novatronics from 1994 to 1996. In 1996, he joined the Electro-Optical Communication Group of Eindhoven University of Technology, Eindhoven, The Netherlands, where he is involved with packaging technologies of integrated optical devices. He was involved in the European research programs ACTS BLISS, ACTS APEX and currently works within IST METEOR.

Giok-Djan Khoe (S'71–M'71–SM'85–F'91) was born in Magelang, Indonesia, on July 22, 1946. He received the degree of Elektrotechnisch Ingenieur (*cum laude*) from the Eindhoven University of Technology, Eindhoven, The Netherlands, in 1971.

He started research at the Dutch Foundation for Fundamental Research on Matter (FOM) Laboratory on Plasma Physics, Rijnhuizen. In 1973, he moved to the Philips Research Laboratories to start research in the area of optical fiber communication systems. In 1983, he was appointed as part-time Professor at Eindhoven University of Technology. He became a full Professor at the same university in 1994 and is currently chairman of the Department of Telecommunication Technology and Electromagnetics. Most of his work has been devoted to single-mode fiber systems and components. Currently his research programs are centered on ultrafast all-optical signal processing, high-capacity transport systems, and systems in the environment of the users. He holds more than 40 U.S. Patents and has authored and coauthored more than 100 papers, invited papers, and book chapters. His professional activities include many conferences, where he has served in technical committees, management committees and advisory committees as a member or chairman. Recently, he was general co-chair of the ECOC 2001. He has been involved in journal activities, as Associate Editor, as a Member of the Advisory Board, or as reviewer. In Europe, he is closely involved with Research Programs of the European Community and in Dutch national research programs, as a participant, evaluator, auditor, and program committee member. He is one of the founders of the Dutch COBRA University Research Institute and one of the three recipients of the prestigious "Top Research Institute Photonics" grant that is awarded to COBRA in 1998 by the Netherlands Ministry of Education, Culture and Science. In 2001, he brought four groups together to start a new international alliance called the European Institute on Telecommunication Technologies (eiTT).

Prof. Khoe he is Associate Editor of the IEEE JOURNAL OF QUANTUM ELECTRONICS. He has served in IEEE Lasers and Electro-Optics Society (IEEE LEOS) organization as European Representative in the BoG, VP Finance & Administration, BoG Elected Member, and member of the Executive Committee of the IEEE Benelux Section. He was founder of the LEOS Benelux Chapter. He received the MOC/GRIN award in 1997. Currently, he was appointed the President-Elect of LEOS in2002.

Huig de Waardt was born in Voorburg, The Netherlands, om December 1, 1953. He received the M.Sc. and Ph.D. degrees in electrical engineering from the Delft University of Technology, Delft, The Netherlands, in 1980 and 1995, respectively.

In 1981 he joined the Department of Physics, KPN Research, Leidschendam, where he was engaged in research on the performance aspects of long-wavelength semiconductor laser diodes, light-emitting diodes, and photodiodes. In 1989, he moved to the Department of Transmission where he has been working in the fields of high-bit-rate direct-detection systems, optical preamplification, wavelength division multiplexing (WDM), dispersion-related system limitations, and the system application of resonant optical amplifiers. He contributed to (inter)national standardization bodies and to the EURO-COST activities 215 and 239. In October 1995 he was appointed an Associate Professor at the University of Eindhoven, Faculty of Electrical Engineering, in the area of high-speed trunk transmission. His current research interests are in applications of semiconductor optical amplifiers, high-speed OTDM transmission, and WDM optical networking. He was active in European research programs as ACTS BLISS, ACTS Upgrade and ACTS APEX. At present he coordinates the TU/e activities in the European projects IST METEOR and IST FASHION. He is member of the project management committee of the national project BTS RETINA. He authored and coauthored more than 60 refereed papers and conference contributions